

In situ net primary productivity and photosynthesis of Antarctic sea ice algal, phytoplankton and benthic algal communities

Andrew McMinn · Andrew Pankowskii ·
Chris Ashworth · Ranjeet Bhagooli ·
Peter Ralph · Ken Ryan

Received: 8 April 2009 / Accepted: 17 February 2010 / Published online: 9 March 2010
© Springer-Verlag 2010

Abstract Primary production at Antarctic coastal sites is contributed from sea ice algae, phytoplankton and benthic algae. Oxygen microelectrodes were used to estimate sea ice and benthic primary production at several sites around Casey, a coastal area in eastern Antarctica. Maximum oxygen export from sea ice was $0.95 \text{ mmol O}_2 \text{ m}^{-2} \text{ h}^{-1}$ ($\sim 11.7 \text{ mg C m}^{-2} \text{ h}^{-1}$) while from the sediment it was $6.08 \text{ mmol O}_2 \text{ m}^{-2} \text{ h}^{-1}$ ($\sim 70.8 \text{ mg C m}^{-2} \text{ h}^{-1}$). When the ice was present O_2 export from the benthos was either low or negative. Sea ice algae assimilation rates were up to $3.77 \text{ mg C (mg Chl-}a\text{)}^{-1} \text{ h}^{-1}$ while those from the benthos were up to $1.53 \text{ mg C (mg Chl-}a\text{)}^{-1} \text{ h}^{-1}$. The contribution of the major components of primary productivity was

assessed using fluorometric techniques. When the ice was present approximately 55–65% of total daily primary production occurred in the sea ice with the remainder unequally partitioned between the sediment and the water column. When the ice was absent, the benthos contributed nearly 90% of the primary production.

Introduction

Antarctic marine coastal primary production is contributed from three main components: sea ice algae, phytoplankton and microalgal and macroalgal benthic communities. Sea ice dominates and structures most Antarctic marine ecosystems (Eicken et al. 1991) and critically limits the amount of light reaching the photosynthetic communities (Palmisano et al. 1985; Smith et al. 1988; Cota and Smith 1991). The sea ice microbial communities are a significant component of the photosynthesizing biomass, contributing approximately 25–30% of annual primary production in perennial ice-covered areas (Legendre et al. 1992; Lizotte 2001; Grose and McMinn 2003). In coastal areas fast ice (i.e. annual ice attached to the shore) has an average biomass of $150 \text{ mg chl-}a \text{ m}^{-2}$, which is mostly located in the bottom 20 cm (Knox 2006) and the production in this community can vary between 0.053 and $1.474 \text{ mg C m}^{-2} \text{ h}^{-1}$ (Trenerry et al. 2002). Beneath the sea ice the phytoplankton biomass remains low ($<0.2 \mu\text{g chl-}a \text{ L}^{-1}$). There are few measurements of Antarctic benthic microalgal biomass, but values between 95 and $960 \text{ mg chl-}a \text{ m}^{-2}$ were reported from McMurdo Sound by Dayton et al. (1986) and between 159.1 and $236.5 \text{ mg chl-}a \text{ m}^{-2}$ at Casey Station by McMinn et al. (2004). The only published Antarctic benthic primary production data comes from the Antarctic Peninsula, where values between 313.4 and

Communicated by K. Yin.

A. McMinn (✉) · A. Pankowskii · C. Ashworth
Institute of Antarctic and Southern Ocean Studies,
University of Tasmania, Private Bag 77,
Hobart, TAS 7001, Australia
e-mail: andrew.mcminn@utas.edu.au

R. Bhagooli · P. Ralph
Institute for Water and Environmental Resource Management,
Department of Environmental Sciences,
University of Technology at Sydney,
Westbourne Street, Gore Hill, NSW 2065, Australia

R. Bhagooli
Department of BioSciences,
University of Mauritius, Reduit, Mauritius

K. Ryan
School of Biological Sciences, Victoria University
of Wellington, PO Box 600, Wellington, New Zealand

700.9 mg C m⁻² d⁻¹ were reported by Gilbert (1991). A comparison of photosynthetic and primary production data among the three major components has not previously been made in Antarctica before, although a comparable study was made in the Beaufort Sea (Horner and Schrader 1982). Because of necessary differences in methodology and units used in the different habitats and the high variability of in situ irradiance and resultant biomass, direct comparisons will always be difficult and prone to inconsistencies.

Advances in the application of microsensor technology to microbial mats have provided new insights and more accurate information than previously available. The application of oxygen microelectrodes to determine oxygen production within sediment, benthic algal communities has been documented over the past 25 years (Jorgensen et al. 1983; Revesbech and Ward 1983; Lorenzen et al. 1995; Klimant et al. 1997). Similar techniques have also been explored to determine productivity of sea ice algal communities (McMinn et al. 2000a; Kuhl et al. 2001; Trenerry et al. 2002; McMinn et al. 2007). This method is based on the measurement of the oxygen flux through the diffusive boundary layer (DBL) (Jorgensen and Revsbech 1985; Roberts and McMinn 2004) and thus allows calculation of the net production of the whole mat (McMinn and Ashworth 1998; McMinn et al. 2000a; Trenerry et al. 2002). The microelectrodes have a fine tip diameter (<40 µm), fast response times to changes in oxygen tension (90% response in <1 s), low stirring sensitivity (<1%) and relatively good long-term stability. They are thus a good tool to investigate the spatial and temporal variability in both production and consumption of O₂ in both the sea-ice and benthic communities.

The development of fluorometric methods for aquatic systems in the mid 1990s has also allowed measurement of marine microalgal photosynthesis and thus estimation of the relative contributions of microalgal groups in aquatic ecosystems. McMinn et al. (2005) documented not only the photo-physiological characteristics of sea ice algal, phytoplankton and benthic algal groups in northern Hokkaido, Japan but also their estimated relative contribution to the coastal production. This method involved the measurement of the maximum relative photosynthetic electron transport rate (rETR_{max}), ambient irradiance and biomass (areal chlorophyll *a* concentration).

The aim of the present study is to examine the diurnal primary productivity of sea ice and benthic algal communities at three sites near Casey Station using oxygen microelectrodes. We also explore the relative contributions of microalgal groups in the three components of the marine Antarctic ecosystem using fluorometric methods.

Materials and methods

Study sites

Field studies were conducted between 2 Dec and 30 Dec 2004 at three sites around Casey Station: Brown Bay (BB), O'Brien Bay (OBB) and Casey Wharf (CW) (66°28'S, 110°52'E) in Antarctica (Fig. 1) Time of day is presented as local time (GMT + 5 h). Measurements of primary production occurred between 3 and 16 December. These sites were chosen as they offer opportunities to work with sea ice (under-ice), phytoplankton (in water column) and benthic (in the sediment) microalgae before and after the annual ice break out. Snow cover in these areas was variable but <0.2 m. Ice thickness (when present) was approximately 1.4 m over the study sites (Table 1). Surface and subsurface irradiance was measured with a Biospherical (San Diego, USA) QSP 200 radiometer with 2π and 4π sensors. Additional irradiance measurements were made with a fibre optic light sensor (after Kuhl et al. 1994) in conjunction with the oxygen microsensor measurements. The weather during the study period was generally overcast but measurements were also made on the less frequent cloud-free days. At Brown and O'Brien Bays, sea ice algae, phytoplankton and benthic algae measurements and collections were made. At Casey Wharf only phytoplankton and benthic algae were studied as no ice remained. Temperature and salinity were measured at each site with a WTW (Weilhelm, Germany) conductivity meter.

Chlorophyll *a* analysis

Chlorophyll *a* (chl-*a*) measurements of sea ice were taken from 4–5 replicate ice cores within a 5 m radius. Ice cores were obtained by drilling a hole to 1.2 m (Jiffy USA) and then extracting the bottom 20–30 cm of core by coring manually with an ice coring drill (Kovaks, USA) to the bottom. The bottom 10 cm of the core sample was removed and trimmed to small blocks before melting them into an equal volume of filtered seawater (0.22 µm filter). 100 ml of the melted sample was filtered onto a Whatman GF/F 47-mm-diameter filter and the pigments were extracted overnight in 10 ml of methanol. A Turner 10 AU fluorometer was employed to measure chlorophyll-*a* biomass following the acidification method of Strickland and Parsons (1972). The fluorometer was calibrated against a chlorophyll-*a* standard (Sigma Chemicals Co., St Louis). While the oxygen flux measurements were measured on a scale of mm, the chl-*a* biomass of the bottom 10 cm was examined. More than 95% of the chl-*a* biomass is typically found in the bottom few centimeters of the sea ice (McMinn et al. 1999, 2000a) and so only this section of ice core was sampled for biomass. Because the ice itself, above

Fig. 1 Location of the three field sites, Casey Wharf, Brown Bay and O'Brien Bay at Casey Station, Antarctica

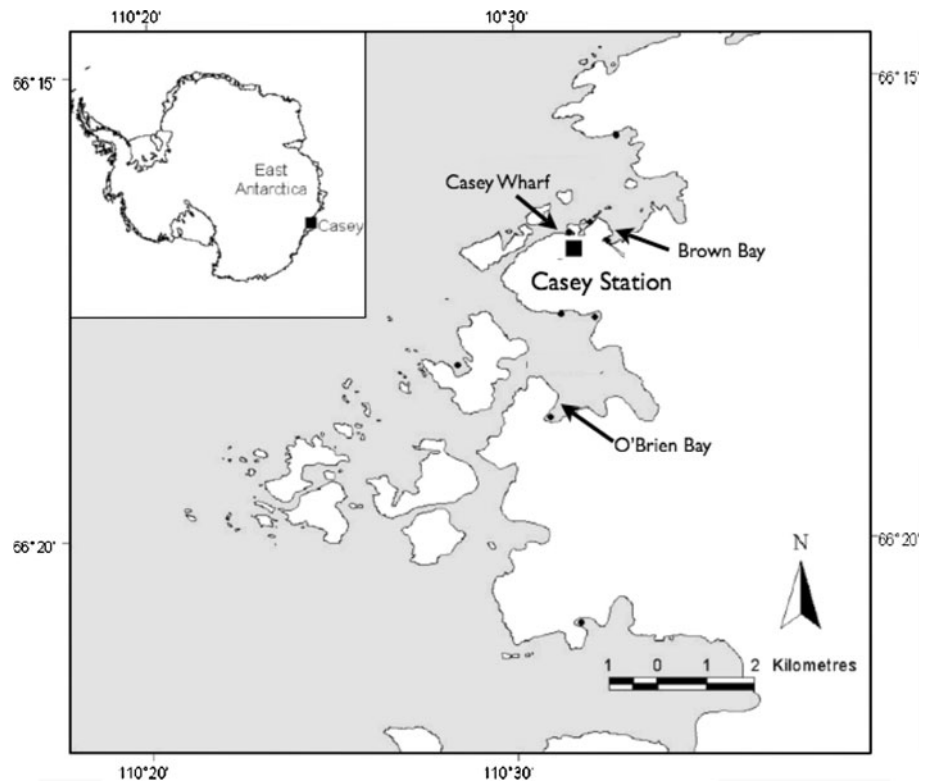


Table 1 Summary of site characteristics

Site	Community	Date	Lat	Long	Ice thickness	Snow depth	Water depth
Brown Bay (BB)	Sea ice algae	12/02	66°16.80'S	110°32.58'E	1.35 ± 0.11	0.15 ± 0.10	8
BB	Benthic algae	12/01	66°16.80'S	110°35.58'E	1.35 ± 0.11	0.15 ± 0.10	8
BB	Phytoplankton	12/02	66°16.80'S	110°35.58'E	1.35 ± 0.11	0.15 ± 0.10	8
O'Brien Bay (OBB)	Sea ice algae	12/09	66°18.72'S	110°30.97'E	1.4 ± 0.15	0.05 ± 0.03	14
OBB	Benthic algae	12/08	66°18.73'S	110°30.99'E	1.4 ± 0.15	0.15 ± 0.03	14
OBB	Phytoplankton	12/10	66°18.73'S	110°30.99'E	1.4 ± 0.15	0.15 ± 0.03	14
Casey Wharf (CW)	Benthic algae	12/30	66°16.46'S	110°33.99'E	–	–	4
CW	Phytoplankton	12/28	66°16.46'S	110°33.99'E	–	–	4

Ice thickness, snow depth and water depth are measured in meters

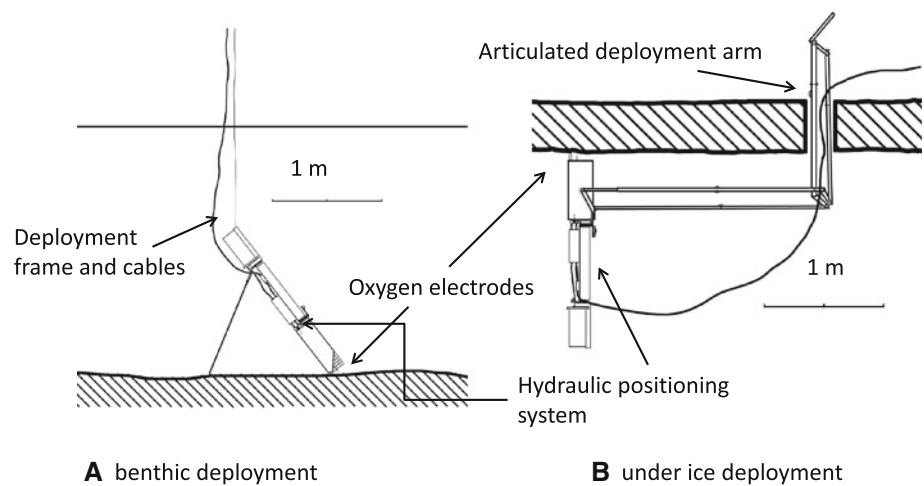
a thin skeletal layer at the ice-water interface, forms an effective cap to vertical oxygen diffusion, it is assumed that all oxygen produced by photosynthesis diffuses down into the diffusive boundary layer (DBL). Therefore, the total biomass of the bottom few cm is required to estimate assimilation numbers. Water column chl-*a* analysis was based on the collection of a 1 L water sample from a depth of 5 m (4 m at Casey Wharf) using a 2 L water sampler (Niskin, USA). The water was subsequently filtered onto Whatman GF/F 47 mm-diameter filters and extracted and analyzed in the same way as the ice cores. Sediment samples for chlorophyll-*a* analysis were collected with a purpose built, 15 mm diameter gravity corer. The top 1 cm of sediment core was removed and pigments extracted in

20 ml of methanol overnight. The resultant chlorophyll extract was decanted and measured in the same manner as the water and ice samples.

In situ net primary productivity

Sea ice and benthic algae net primary production was measured using the in situ oxygen flux across the DBL method (Jorgensen and Revsbech 1985; McMinn et al. 2000a). The equipment and oxygen microelectrodes (Uni-Sense, Aarhus), that were deployed to take the in situ measurements of sea ice and benthic algae, were a modification of the equipment used by McMinn et al. (2000a) and Trenerry et al. (2002) (Fig. 2). Both the flux of oxygen

Fig. 2 Oxygen microelectrode deployment equipment. The same hydraulic microelectrode positioning system was used for both benthic (a) and under ice (b) deployment. In the under ice deployment mode, light, oxygen temperature and salinity sensors are located together. During benthic deployment, the light sensor remains above the sediment surface. Video equipment is located within the hydraulic structure



from beneath the sea-ice algal mat or above the sediment algal layer and the thickness of the DBL are necessary to determine the net primary productivity. Oxygen concentration was measured with oxygen microelectrodes that had a tip diameter of approximately 40 μm , a 90% response time of approximately 1 s and a stirring sensitivity of 1–2%. They were calibrated on site immediately prior to measurement using values from air-saturated seawater (saturated by bubbling with a standard aquarium pump for 20 min at -1.8°C) and for deoxygenated seawater (using sodium sulphite at -1.8°C). Oxygen concentration values, in $\mu\text{mol O}_2 \text{ L}^{-1}$, for air saturated seawater at -1.8°C were obtained from Weiss (1970). Measurement of both the DBL thickness and the oxygen flux was carried out by stepping the oxygen microelectrode at 10 μm intervals through the first few millimeters of water under ice or above the sediment. While for sea ice measurements the equipment was deployed beneath the sea ice on extendable arms (McMinn et al. 2000a), for benthic measurements the equipment was lowered to a resting position with cables and subsequently remained in communication with a computer at the surface (Fig. 2).

The fibre-optic light sensor, which was constructed after Kuhl et al. (1994), was compared with a Biospherical QSP 200 4π PAR sensor and a linear relationship across a range of subsurface irradiances was obtained. Light measurements were made just beneath the sea ice and just above the sediment algal mats, for sea ice and benthos measurements respectively. The light sensor had a maximum detectable light level of approximately 71 $\mu\text{mol photons m}^{-2} \text{ s}^{-1}$, resulting in some readings at Casey Wharf and O'Brien Bay exceeding the maximum. For these measurements the ambient underwater irradiance was calculated from surface light levels and extinction coefficients determined from that part of the water column which had irradiance levels less than 71 $\mu\text{mol photons m}^{-2} \text{ s}^{-1}$. Light, oxygen and position data were logged onto a PC at

the surface approximately every second. Recognition of the bottom of the sea ice DBL was with repeated O_2 values or by a rapid decline in O_2 concentration associated with touching the ice. The bottom of the DBL in the sediment was recognized by a distinct change in slope of the oxygen flux associated with a diffusional rate change as the microelectrode entered the sediment (Fig. 3). The top of each DBL was calculated by determining the depth at which there had been an increase of 10% of the total change in oxygen concentration (i.e. the oxygen export equivalent of the 90% of free-flow concentration of Jorgensen and Marais 1990; Trenerry et al. 2002). Underwater video cameras were positioned 5 m from the measuring equipment and 10 cm from the electrode tip to ensure proper deployment of the equipment had occurred. Full DBL profiles of sea ice and sediments were obtained every 15-min for 24 h in sea ice and 12 h in sediments. Sea ice productivity measurements were made prior to significant ice melt to ensure the dominant mode of oxygen transfer was by diffusive rather than advective processes. As sea ice melts a layer of fresher water often develops beneath the ice (Cota and Horne 1989; Kuhl et al. 2001) and similarly, as ice forms, brine is excluded from the ice creating a flux of high salinity water. The development of these gradients has the potential to significantly influence the transport of solutes across the ice water interface (Glud et al. 2002a, b). However, at Casey during this time there was no detectable change in ice thickness over the experimental period, the temperature remained between -1.7 and -1.8°C and the salinity did not vary. This indicates that diffusive rather than convective molecular transport was responsible for most of the measured oxygen flux and validates our approach. This method, however, would not be appropriate if the ice was either rapidly growing or melting.

The oxygen diffusion flux (J) across the DBL is equivalent to the net primary productivity of the algal mat either under ice or above the sediment. It was calculated

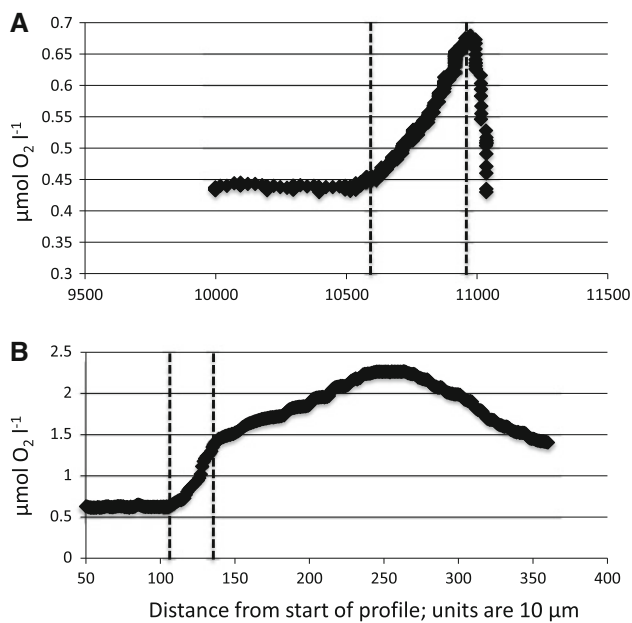


Fig. 3 Examples of oxygen profiles of the diffusive boundary layer (DBL) obtained from oxygen microelectrode measurements of **a** sea ice (Brown Bay at 2:44 pm, 2 December 2004) and **b** benthic algal communities (Casey Wharf at 2:14 pm, 1 December 2004). Vertical scale represents diffusive oxygen flux, horizontal scale is the distance in microns from the start of the profile. The diffusive boundary layer is marked by dashed lines

using the 1-dimensional version of Fick's first law of diffusion (Revsbech and Jørgensen 1986):

$$J = D_o(d[O_2]/dx)$$

where D_o = molecular diffusion coefficient (at -1.9°C = $1.11 \times 10^{-5} \text{ cm}^{-2} \text{ s}^{-1}$); Broecker and Peng 1974), dx = DBL thickness, $d[O_2]$ = change in oxygen concentration across the DBL. To convert oxygen fluxes into equivalent net productivity values the oxygen flux ($\text{mmol O}_2 \text{ m}^{-2} \text{ h}^{-1}$) was divided by a photosynthetic coefficient for Antarctic fast ice of 1.03 (Satoh and Watanabe 1988) and multiplied by the atomic weight of carbon (12.01). This value is equivalent to production in $\text{mg C m}^{-2} \text{ h}^{-1}$. The assimilation number was obtained by dividing the 'carbon equivalent' productivity value by the chlorophyll value to give units of $\text{mg C (mg chl-}a\text{)}^{-1} \text{ h}^{-1}$. This change to a carbon equivalent assimilation number was made to enable comparisons with productivity estimates made using more familiar ^{14}C methods.

Chlorophyll fluorescence measurements

Chlorophyll fluorescence of sea ice algae, phytoplankton and benthic algae were measured using a pulse-amplitude-modulated fluorometer (Water-PAM, Waltz, Effenberg, Germany). The initial fluorescence (F) was measured by applying a weak measuring light ($<1 \mu\text{mol photons}$

$\text{m}^{-2} \text{ s}^{-1}$) and a saturating pulse ($>3,000 \mu\text{mol photons m}^{-2} \text{ s}^{-1}$ for 0.8 s) was applied to determine the maximum fluorescence (F_m'). The ratio of the change in fluorescence ($\Delta F = F_m' - F$) and the maximal fluorescence, $\Delta F/F_m'$, is a measure of the effective quantum yield of PSII in the illuminated sample. The relative photosynthetic electron transport rate (rETR) was calculated as the product of the effective quantum yield and quantum flux density of photosynthetically active radiation (PAR) (Genty et al. 1989).

All samples were taken as close as possible to midday. Care was taken to ensure that the samples were not exposed to direct sunlight. Sea ice algae were shaved off the bottom of ice cores and placed in the measuring cuvette of the Water-PAM with 1–2 ml of -1.8°C filtered seawater (McMinn et al. 2005). The ice was not melted. This method of measurement has the advantage of not melting the ice and exposing the cells to osmotic and temperature shocks while making no significant difference to subsequent quantum yield measurements. Sediment samples (top 5 mm of each sediment core) were collected with a small gravity sediment corer, with 15 mm diameter tubes, and again carried under black plastic into a tent and placed into the measuring cuvette. Sea-water was collected from 5 m under the ice. To obtain the rapid light curves (RLC), samples in the measuring cuvette were light-acclimated (to an irradiance as close as possible to ambient, i.e. approx $10\text{--}20 \mu\text{mol photons m}^{-2} \text{ s}^{-1}$) for 5 min using the internal actinic light source of the PAM fluorometer. After 30 s of darkness, rapid light curves were obtained by illuminating the samples for 10 s before each $\Delta F/F_m'$ measurement at each of a series of eight irradiances that increased in steps from 0 to $577 \mu\text{mol photons m}^{-2} \text{ s}^{-1}$ (White and Critchley 1999; Ralph and Gademann 2005). Light was provided by the internal actinic light source, which in the WaterPAM is centred on 660 nm.

The rETR data generated by the rapid light curves were fitted to the following equation with a multiple non-linear regression (Platt et al. 1980):

$$\text{rETR} = \text{rETR}_{\text{max}} [1 - \exp(-\alpha E_d / \text{rETR}_{\text{max}})] \times \exp(-\beta E_d / \text{rETR}_{\text{max}})$$

rETR_{max} represents the maximum potential rETR in the absence of photoinhibition. α is the initial slope of the light curve before the onset of saturation and represents the efficiency of light utilization. E_d is the irradiance (in the general formula 400–700 nm). β is the parameter characterizing photoinhibition. In the absence of photoinhibition in the light curves, where $\beta = 0$, the function becomes:

$$\text{rETR} = \text{rETR}_{\text{max}} [1 - \exp(-\alpha E_d / \text{rETR}_{\text{max}})]$$

where rETR_{max} is the maximum rETR at light saturation and thus represents the photosynthetic capacity. Standard

RLCs only generate 9 points in their P vs. E function, unlike traditional ^{14}C -based P vs. E functions, which typically have 20 or more data points (Lewis and Smith 1983). This low number of data points makes correctly estimating both alpha and beta unreliable. Therefore, because none of the communities in this study were inhibited at their maximum ambient irradiance, we removed any ‘inhibited’ data points (rarely more than one per RLC) from the multiple non linear regressions. In this way we achieved a more robust estimate of rETR_{max} and α .

Contribution of phytoplankton, sea ice algae and benthic algae

The relative contribution of phytoplankton, sea ice algae and benthic algae were calculated as in McMinn et al. (2005), i.e. by multiplying the areal (m^{-2}) chl-*a* concentration of each component by their respective rETR at its maximum ambient irradiance.

$$\text{Total productivity} = (\text{Chl-}a_{\text{phyt}} \times \text{rETR}_{\text{phyt}}) + (\text{Chl-}a_{\text{sia}} \times \text{rETR}_{\text{sia}}) + (\text{Chl-}a_{\text{ba}} \times \text{rETR}_{\text{ba}})$$

Relative production of sea ice algae

$$= (\text{Chl-}a_{\text{sia}} \times \text{rETR}_{\text{sia}}) / \text{Total productivity}$$

where phyt = phytoplankton, sia = sea ice algae and ba = benthic algae.

This approach does not take into account light gradients within each of the microenvironments or diurnal diatom migration patterns. Instead it uses an average photosynthetic response from the RLCs and spot measurements for biomass calculations. Nevertheless, as each community is largely dominated by the same diatom species, it still gives a first order impression of the relative contribution of each community.

Results

Physical and biological site parameters are summarized in Table 1. Chl-*a* biomass during oxygen electrode experimentation was variable among sites. Sea ice, benthic and phytoplankton chl-*a* at O’Brien Bay (OBB) was approximately 50, 65 and 3 fold, respectively, higher than that at Brown Bay (BB). The benthic and phytoplankton chl-*a* biomass at Casey Wharf (CW) was almost 3 times higher than that at O’Brien Bay. Benthic chl-*a* biomass was generally the highest ($\text{CW} = 186 \pm 146$, $\text{OBB} = 71.5 \pm 63.3$, $\text{BB} = 1.10 \pm 0.55 \text{ mg chl-}a \text{ m}^{-2}$) of the three sampled ecosystem components (Table 1). The water temperature beneath the ice during the experimentation time remained around -1.9°C for the sea ice and benthos, while it rose to -1.7°C after the ice broke out. The ice thickness

was approximately 1.4 m at BB and OBB, while at CW it had already melted prior to the sampling period.

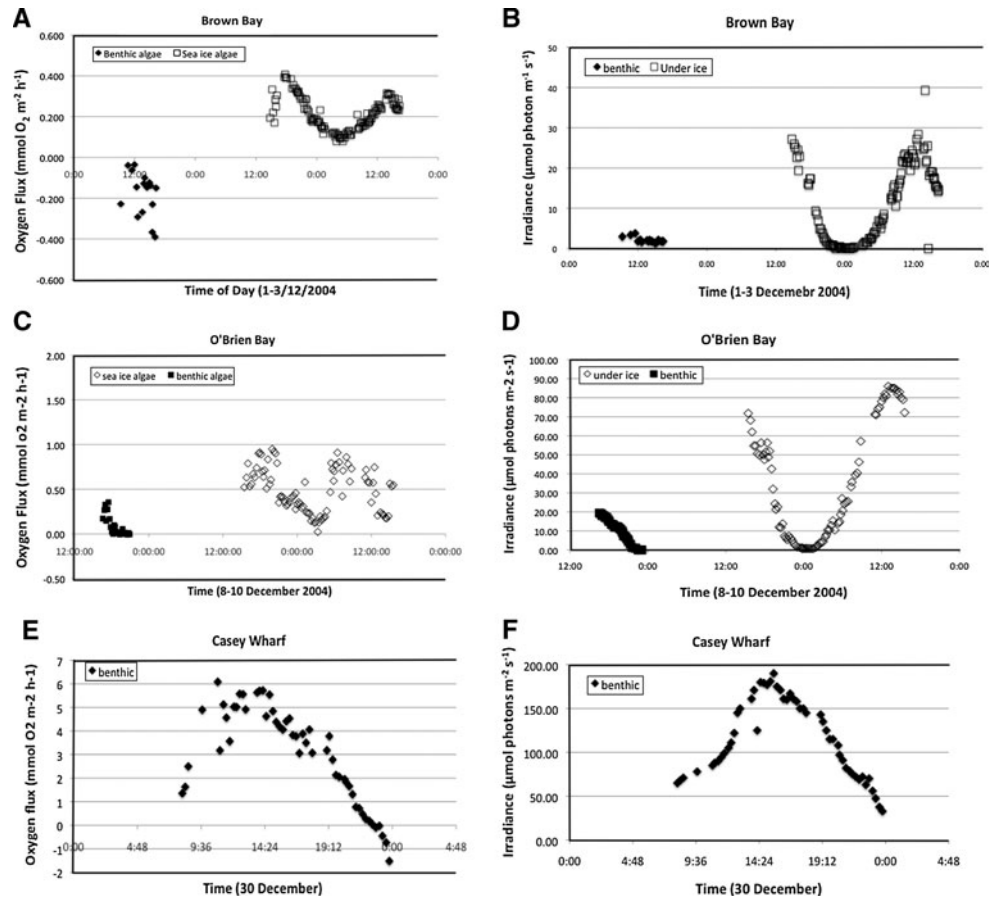
Oxygen profiles from sea ice and sediment DBL measurements were obtained between 2 and 30 December 2004. Examples of both under-ice and sediment profiles are given in Fig. 3. Peak light levels beneath the sea ice and above the sediment at BB were 39 and $4.6 \mu\text{mol photons m}^{-2} \text{ s}^{-1}$ (Fig. 4b). At OBB the under-ice light levels peaked at approximately $86 \mu\text{mol photons m}^{-2} \text{ s}^{-1}$ and above the sediment at $19.4 \mu\text{mol photons m}^{-2} \text{ s}^{-1}$ (Fig. 4e). The highest recorded benthic light level at the CW site was $191 \mu\text{mol photons m}^{-2} \text{ s}^{-1}$ (Fig. 4g). Under-ice light levels were approximately eightfold higher than benthic light levels at BB and 4 times higher in OBB.

The under-ice net oxygen export was generally higher at OBB (maximum $0.95 \text{ mmol O}_2 \text{ m}^{-2} \text{ h}^{-1}$, minimum $0.00216 \text{ mmol O}_2 \text{ m}^{-2} \text{ h}^{-1}$ Fig. 4c) than at BB (maximum $0.406 \text{ mmol O}_2 \text{ m}^{-2} \text{ h}^{-1}$, minimum $0.00792 \text{ mmol O}_2 \text{ m}^{-2} \text{ h}^{-1}$, Fig. 4a). The maximum benthos net oxygen export was $0.350 \text{ mmol O}_2 \text{ m}^{-2} \text{ h}^{-1}$ and the minimum was a net influx of $0.0446 \text{ mmol O}_2 \text{ m}^{-2} \text{ h}^{-1}$ at OBB (Fig. 4c). There was a consistent net benthos oxygen influx at BB, which varied between $(-)$ $0.0385 \text{ mmol O}_2 \text{ m}^{-2} \text{ h}^{-1}$ and $(-)$ $0.390 \text{ mmol O}_2 \text{ m}^{-2} \text{ h}^{-1}$. At CW, the benthos net oxygen export was at a maximum of $6.08 \text{ mmol O}_2 \text{ m}^{-2} \text{ h}^{-1}$ and a minimum of $1.51 \text{ mmol O}_2 \text{ m}^{-2} \text{ h}^{-1}$ (Fig. 4e). There was a substantial increase in the diurnal production rates in the benthos when the ice was absent (CW) compared to when the ice was present (at BB and OBB).

The ‘carbon equivalent’ assimilation numbers of the sea ice algae at BB and OBB was at a maximum of 0.15 and $3.77 \text{ mg C (mg chl-}a)^{-1} \text{ h}^{-1}$ respectively and at a minimum of 0.0043 and $0.73 \text{ mg C (mg chl-}a)^{-1} \text{ h}^{-1}$ respectively. The maximum and minimum assimilation rates of the benthos at OBB, BB and CW were 1.53, -1.08 , $0.38 \text{ mg C (mg chl-}a)^{-1} \text{ h}^{-1}$, and -5.19 , -7.08 , $-0.09 \text{ mg C (mg chl-}a)^{-1} \text{ h}^{-1}$ respectively.

Maximum quantum yields of the different ecosystem components varied between sites (Table 2). At BB the sea ice algae had the highest Fv/Fm (0.668) followed by the phytoplankton (0.586) and the benthos (0.543). At OBB the benthos value was highest (0.587) followed by the phytoplankton (0.546) and the sea ice algae (0.485). There was a significant difference ($P < 0.05$, $n = 5$) between Fv/Fm of the sea ice, the benthos and the phytoplankton at BB. At OBB the Fv/Fm of the benthos was significantly different ($P < 0.05$, $n = 5$) from both the sea ice algae and the phytoplankton but the latter were not significantly different from each other. At CW the Fv/Fm of the benthos and phytoplankton were also significantly different ($P < 0.05$, $n = 5$). The maximum relative electron transport rates (rETR_{max}) were between 32–64 (Table 2). At Brown Bay

Fig. 4 Diurnal production ($\text{mmol O}_2 \text{ m}^{-2} \text{ h}^{-1}$) and irradiance ($\mu\text{mol photons m}^{-2} \text{ s}^{-1}$) at Brown Bay (BB) on 2 December, **a, b** O'Brien Bay (OB) on 10 December, **c, d** and Casey Wharf (CW) on 30th December, **e, f**



the rETR_{max} for the ice algae, benthos and phytoplankton were not significantly different ($P < 0.05$), being 31.9 ± 2.6 , 37.2 ± 7.7 , 33.5 ± 4.0 respectively. At OBB, although the values were higher, i.e. 43.8 ± 5.2 , 40.8 ± 3.7 , 50.3 ± 13.2 respectively, there were still no significant differences ($P < 0.05$). The rETR_{max} values from CW, after the ice break out were higher, benthos = 46.5 ± 5.4 , phytoplankton = 63.6 ± 12.6 , and significantly different from each other ($P < 0.05$). There were significant differences ($P < 0.05$) between the α values, i.e. the photosynthetic efficiency, of the different components at each site (Table 2). At BB the benthos had the highest α value followed by the sea ice algae and then the phytoplankton. At OBB the phytoplankton had the highest value followed by the benthos and the ice algae. At CW the benthos had a much higher α value than the phytoplankton.

While it wasn't possible to measure productivity of all three components using the DBL method, the reliability of using the PAM method to compare relative contributions can be assessed by comparing the ratio of sea ice algae to benthic algae production by both methods. In OBB the ratio of sea ice algae to benthic algae production using DBL methods was 2.71 (i.e. 0.95:0.35). Using the PAM

method, i.e. $\text{chl-}a \times \text{rETR}$, the ratio was 2.43 (i.e. $1687.8 (27.4 \times 61.6 \text{ mg chl-}a \text{ m}^{-2})$: $693.6 (9.7 \times 71.5 \text{ mg chl-}a \text{ m}^{-2})$), which was quite similar to the ratio estimated by the DBL method. This comparison was not possible at BB because there was no net oxygen export and at CW because there was no ice cover.

The WaterPAM was employed to estimate the relative contributions to primary production by the sea ice algae, phytoplankton and benthic algae (Table 2). When sea ice was present, sea ice algae made the largest contribution to primary productivity (BB and OBB). When sea ice was absent (CW) benthic algae made the largest contribution. The phytoplankton never made the largest contribution.

Discussion

Primary production of the three Antarctic/Arctic marine ecosystem components of primary production has usually been reported separately and in different studies. The relative contribution of the three primary production components in polar environments is still debatable and has been difficult to quantify due to inherent spatio-temporal variability and methodological inconsistency resulting in less

Table 2 Photosynthetic parameters and productivity of the three Casey sites

	Fv/Fm	rETR _{max}	α	E _k	Ox. export	AN
Brown Bay 3-Dec-2004						
Sea ice algae	0.668 ± 0.009	31.9 ± 2.6	0.534 ± 0.054	60 ± 8	0.406	0.15
Phytoplankton	0.586 ± 0.021	33.5 ± 5.96	0.359 ± 0.169	137 ± 100		
Benthic algae	0.543 ± 0.009	37.2 ± 7.67	0.686 ± 0.230	50 ± 16	n/a	n/a
O'Brien Bay 10-Dec-2004						
Sea ice algae	0.485 ± 0.042	43.8 ± 5.19	0.511 ± 0.012	89 ± 20	0.95	3.77
Phytoplankton	0.546 ± 0.042	50.3 ± 13.2	0.852 ± 0.111	61 ± 22		
Benthic algae	0.587 ± 0.007	40.8 ± 3.7	0.641 ± 0.067	67 ± 12	0.351	1.53
Casey Wharf 30-Dec-2004						
Phytoplankton	0.574 ± 0.002	46.5 ± 5.4	0.599 ± 0.034	78 ± 12	6.08	0.38
Benthic algae	0.545 ± 0.021	63.6 ± 12.6	0.378 ± 0.057	171 ± 46		

Errors are standard deviations based on 7 replicate samples. Ox. export is oxygen export ($\text{mmol O}_2 \text{ m}^{-2} \text{ h}^{-1}$), Negative oxygen flux is indicated with n/a. AN is the 'carbon-equivalent' assimilation number ($\text{mg C (mg chl-}a\text{)}^{-1} \text{ h}^{-1}$)

reliable comparative estimates. Recently, however, a comprehensive carbon budget for an east Greenland fjord was produced that examined all these components using consistent approaches (Rysgaard and Glud 2007). They estimated that phytoplankton contributed 65% of the annual primary production, benthic microalgae 21% and sea ice algae less than 1%. In west Greenland Mikkelsen et al. (2008) likewise concluded that while sea ice algae made a major contribution to primary production in spring and summer, over a year it contributed less than 1% of the total. Here we present combined in situ production and relative contribution data from the sea ice algal, phytoplankton and benthic algal communities at three sites near Casey Station, Antarctica.

McMinn et al. (2000a) and Trenerry et al. (2002) presented in situ oxygen microelectrode data measured from Antarctic fast ice algal communities. Other sea ice microelectrode measurements of productivity have been presented by McMinn and Hegseth (2004), and (2007) from Antarctic pack ice, by Rysgaard et al. (2001) and Kuhl et al. (2001) from Arctic fast ice and McMinn and Hegseth (2006) from Arctic pack ice. Maximum sea ice primary productivity at Casey in spring 2004 was $3.77 \text{ mg C (mg chl-}a\text{)}^{-1} \text{ h}^{-1}$ in O'Brien Bay and $0.46 \text{ mg C (mg chl-}a\text{)}^{-1} \text{ h}^{-1}$ in Brown Bay. This compares with values of $0.29\text{--}2.01 \text{ mg C (mg chl-}a\text{)}^{-1} \text{ h}^{-1}$ from spring 1997 (McMinn et al. 2000a) and $0.0059 \text{ mg C (mg chl-}a\text{)}^{-1} \text{ h}^{-1}$ from spring 1999 in McMurdo Sound (Trenerry et al. 2002).

There have been very few previous measurements of benthic primary production in any polar areas and only two, Kuhl et al. (2001) and Glud et al. (2002a, b) that used oxygen microelectrode methods. In the Casey area maximum light levels at the sediment surface when sea ice was

present were low, only $2.68 \mu\text{mol photons m}^{-2} \text{ s}^{-1}$ at BB and $19.4 \mu\text{mol photons m}^{-2} \text{ s}^{-1}$ at OBB and consequently rates of oxygen efflux were also very low, in fact mostly negative. These low rates almost certainly represent net community respiration from bacteria and micro zoobenthos as it is difficult to envisage an algal community suffering such extensive respiratory losses for the nine months they are potentially covered by sea ice. After ice break out, sediment surface light levels reached a maximum of over $190 \mu\text{mol photons m}^{-2} \text{ s}^{-1}$ at Casey Wharf (CW) and production increased to over $6.08 \text{ mmol O}_2 \text{ m}^{-2} \text{ h}^{-1}$ ($\sim 66 \text{ mg C m}^{-2} \text{ h}^{-1}$). In the only other comparable study Kuhl et al. (2001) reported primary production from a benthic diatom mat in a Greenland fjord to be approximately $100 \text{ mmol O}_2 \text{ m}^{-2} \text{ d}^{-1}$, which compares with a value of $\sim 36.5 \text{ mmol O}_2 \text{ m}^{-2} \text{ d}^{-1}$ at Casey Wharf. These production levels at Casey Wharf, although high even compared to values from temperate areas, reflect the high benthic microalgal biomass. Benthic microalgal biomass values from the Greenland study (Kuhl et al. 2001) were not reported. The only other known measurements of polar coastal benthic primary production are $13.06\text{--}29.17 \text{ mg C m}^{-2} \text{ h}^{-1}$, at Signy Island on the Antarctic Peninsula (Gilbert 1991) and $<0.01\text{--}0.07 \text{ mg C m}^{-2} \text{ h}^{-1}$ from the Arctic Beaufort Sea (Horner and Schrader (1982) determined using ^{14}C methods.

It is probable that differences between the PAM-based photosynthetic parameters of BB, OBB and CW mostly reflected the increasing light levels as the sea ice broke out (Table 2). The Fv/Fm of the phytoplankton samples decreased from 0.586 ± 0.021 on 3-Dec, to 0.546 ± 0.056 on 10-Dec to 0.278 ± 0.028 on 16-Dec. During the same period the rETR_{max} of the water incrementally increased from 33.5 ± 5.9 to 63.6 ± 12.6 . The Fv/Fm values of the

benthos remained approximately constant at ~ 0.56 while the $rETR_{max}$ values also incrementally increased from 37.2 ± 7.7 to 46.5 ± 5.4 . The sea ice samples did not show a clear trend. However, as these values were collected from different, albeit nearby, sites, interpretations should be treated with caution. These measurements were all taken as close as possible to midday, a time when the photosystems of these organisms are known to experience down regulation or photoinhibition (McMinn et al. 2003). Even though the samples were dark adapted for 15 min prior to measurement, this period was probably insufficient for full recovery as some recovery processes take minutes to hours to complete (Beardall et al. 2009) and this is reflected in the relatively low maximum quantum yields.

Benthic algae photosynthetic parameter values documented here are mostly consistent with those recorded by McMinn et al. (2004) from the same area. While F_v/F_m , E_k , α and $rETR_{max}$ (before ice break out) are comparable, in the 2003 study (McMinn et al. 2004) $rETR_{max}$ after ice break was considerably higher. However, as no taxonomic comparisons can be made it is not possible to determine the cause.

A quantitative assessment of phytoplankton production was not made. Instead, relative production was estimated by measuring relative electron transport ($rETR$) using PAM RLCs. This allowed a direct comparison between benthic, sea ice and pelagic microalgal productivity to be made. The validity of using this approach was tested by comparing the ratio of sea ice algae and benthic algae production at OBB using the two different methods. Using the DBL method the ratio of sea ice production to benthic algae production was 2.71; using the PAM method the ratio was a similar 2.43. The ratio at BB could not be compared as oxygen output from the benthos remained negative. The two methods, however, do not measure the same photosynthetic parameters. The DBL method measures net community productivity, while the PAM method measures gross photosynthesis and so does not include respiratory losses. As the proportion of production lost due to respiration will be greater at lower light levels, the slightly lower ratio estimated by the PAM method at OBB is consistent and demonstrates that the PAM method provides a realistic estimate of the relative contribution of at least the benthic microalgae and sea ice algae components and probably, by extension, also the phytoplankton.

Microalgal production is a function of biomass, irradiance and photosynthetic physiology. Biomass and irradiance typically vary over several orders of magnitude while physiological factors, such as maximum quantum yield of photosynthesis, quantum efficiency, photosynthetic quotients etc., vary on a much smaller scale. Consequently, light and biomass differences have a much larger effect on primary production measurements than physiological

differences. Furthermore, because biomass is the most variable parameter in the measurement of productivity, it is sometimes used as a proxy for productivity. However if this were done at Casey it would sometimes lead to a misinterpretation of the relative contribution of the three microalgal components. For example, in BB the phytoplankton has the largest biomass, followed by the sea ice algae and the benthic algae but because of higher irradiances in the ice, this component contributes the most to productivity. At the other two sites, differences in biomass between the components is much greater and those with the greatest biomass have the greatest contribution.

It is often not appropriate to directly compare $rETR$ s of different communities because different microalgal communities are likely to have differing taxonomic compositions, with differing pigment complements. Microalgal taxa also have differing absorption cross-sectional area of PSII and display differing ratios between electrons generated in PSII (proportional to fluorescence) and oxygen synthesis, both of which also vary with acclimation status (Flameling and Kromkamp 1998). However, in Antarctic coastal environments the communities are often closely coupled and in springtime are all dominated by diatoms and often by the same species (McMinn et al. 2000b, 2005). It is likely therefore, that when the productivity measurements were taken before ice break out (i.e. at OBB and BB but not CW), melting sea ice contributed a significant proportion of the microalgal cells to the benthic microalgae and possibly the phytoplankton. While species identifications were not made at the time, earlier studies have shown that sea ice-derived microalgae make an important contribution to benthic microalgal biomass (McMinn et al. 2004; Cunningham and McMinn 2004) but only a minor contribution to the phytoplankton (McMinn and Hodgson 1993; McMinn 1996; McMinn et al. 2000a, b). In a study in northern Hokkaido McMinn et al. (2005) estimated the relative contribution of sea ice algae, phytoplankton and benthic microalgae by summing the product of the chl-*a* biomass and $rETR$ at the maximum ambient environmental irradiance of each photosynthetic component. They found that even though the greatest microalgal biomass was in the sediments the greatest contribution to primary production (54.3%) came from the sea ice microalgae. Horner and Schrader (1982), using ^{14}C methods in the ice covered Beaufort Sea in spring, similarly found $\sim 65\%$ of primary production was from the sea ice, $\sim 35\%$ from the water column and only a negligible proportion from the benthos.

The contribution from the three photosynthetic components in the Casey area in December (2004) varied depending on site and the ice state (Table 2). When the ice was present, ice algae contributed between 57.1 and 64.6% of the total. When the ice was absent the contribution from

the benthos became increasingly important, up to 89.8%. These results are predictable in a light-limited environment such as under sea ice. The amount of light penetrating Antarctic fast ice to the underlying water column varies depending on ice thickness, snow cover and internal biomass. In springtime maximum under ice irradiance has varied between from as little as $0.5 \mu\text{mol photons m}^{-2} \text{s}^{-1}$ (McMinn et al. 1999) to as much as $55 \mu\text{mol photons m}^{-2} \text{s}^{-1}$ (McMinn et al. 2000a). While most of these sea ice algal communities show extreme dark adaptation (Arrigo 2003), they often remain light-limited for much of the day (Trenerry et al. 2002). However, once the ice has broken out the light limitation is reduced and there is strong evidence that the phytoplankton then become nutrient-limited during late spring and summer (McMinn et al. 1995, 2000b). Benthic microalgal communities, on the other hand, while receiving less light are less likely to become nutrient limited because of their slower growth and strong association with remineralizing microbial communities at the sediment surface (Dalsgaard 2003, Blackburn et al. 1996, Glud et al. 1998). Although temporal trends in the nutrient status of Antarctic benthic microalgae have not yet been established, it is reasonable to assume they function in a similar manner to such communities elsewhere. Horner and Schrader (1982) were the first to estimate the relative contribution of phytoplankton, sea ice algae and phytobenthos to total primary production in polar areas. Their study indicated that sea ice algae contributed two-thirds of the total in spring and early summer. More recently a comprehensive examination of carbon cycling in Young Sound, east Greenland found that while sea ice production was important during spring, contributing up to one-third of total primary production, over a year it contributed less than 1%. In the Antarctic the contribution of sea ice to annual primary production is estimated to be 25–30% in the pack ice (Legendre et al. 1992; Arrigo and Thomas 2004) and probably greater in the fast ice where ice cover extends for a longer period (Table 3).

Climate change is likely to alter the future development and importance of the different components of Antarctic coastal marine primary production (Arrigo and Thomas 2004). With sea ice melting and breaking up earlier, ice algal production is likely to decrease. The early disappearance of the ice could lead to earlier spring phytoplankton blooms, but as these coastal blooms already become nutrient limited by mid summer (McMinn et al. 1995, 2000), their earlier development could also lead to an earlier demise. Maximum benthic microalgal development currently, probably occurs after light to the bottom increases following both ice break out and increasing water transparency due to bloom decline. Because these communities have access to remineralised nutrients from the sediments, they are less likely to become nutrient-limited

Table 3 Relative proportion of sea ice algae, phytoplankton and benthic algae primary production

	Biomass	E _{max}	rETR	%
Brown Bay 3-Dec-2004				
Sea ice	1.26 ± 0.71	39	15.4	57.1
Phytoplankton (5 m)	3.15 ± 0.21	10.3	4.1	38.0
Benthic algae (8 m)	1.1 ± 0.04	4.6	1.5	4.9
O'Brien Bay 10-Dec-2004				
Sea ice	61.64 ± 15.56	86	27.4	64.6
Phytoplankton (5 m)	9.87 ± 1.43	51	23.5	8.9
Benthic algae (14 m)	71.5 ± 63.31	19.4	19.4	26.5
Casey Wharf 30-Dec-2004				
Phytoplankton (4 m)	24.87 ± 2.09	191	29.3	10.2
Benthic algae (4 m)	186.83 ± 146	191	34.3	89.8

Biomass is in $\text{mg chl-}a \text{ m}^{-2}$ ($n = 3$), E_{max} is the maximum ambient irradiance at each habitat ($\mu\text{mol photons m}^{-2} \text{s}^{-1}$), rETR is the mean ($n = 5$) relative electron transfer rate (ETR) at E_{max}, % is the relative proportion each community contributes to total productivity

and hence are likely to develop earlier and continue longer. Hence, it is probable that in a future Antarctic coastal environment where ice forms later and melts earlier, benthic microalgal primary production will become a larger component of net production. Our study has made a preliminary attempt to quantify both the extent of sea ice and benthic production and estimate the relative contribution from these components and from phytoplankton. This data will provide a useful snapshot to assess future environmental change.

In summary, Antarctic coastal primary production is derived from sea ice algae, phytoplankton and benthic microalgae and for a short period these communities can be highly productive. The presence of sea ice controls where most primary production occurs. When the ice is present approximately 55–65% of production occurs in sea ice with the remainder partitioned between the sediment and the water column. When the ice is gone, the benthos can contribute up to 90% of the production.

Acknowledgments We acknowledge the financial support of ARC and AAS to Andrew McMinn and Peter Ralph and logistical support from the Australian Antarctic Division.

References

- Arrigo KR (2003) Primary production in sea ice. In: Thomas DN, Dieckmann GS (eds) *Sea Ice; an introduction to its physics, chemistry, biology and geology*. Blackwell Science, Oxford, pp 143–183
- Arrigo KR, Thomas DN (2004) Large scale importance of sea ice biology in the Southern Ocean. *Antarctic Sci* 16:471–486
- Blackburn TN, Hall POJ, Hulth S, Landen A (1996) Organic-N loss by efflux and burial associated with low efflux of inorganic N

- and nitrate assimilation in Arctic sediments (Svalbard, Norway). *Mar Ecol Prog Ser* 141:283–293
- Broecker WS, Peng TH (1974) Gas exchange rates between air and sea. *Tellus* 26:21–35
- Cota FG, Horne EPW (1989) Physical control of Arctic ice algal production. *Mar Ecol Prog Ser* 52:111–121
- Cota FG, Smith REH (1991) Ecology of bottom ice algae: III. Comparative physiology. *J Mar Syst* 2:297–315
- Cunningham L, McMinn A (2004) The influence of natural environmental factors on benthic diatom communities from the Windmill Islands, Antarctica. *Phycologia* 43:744–756
- Dalsgaard T (2003) Benthic primary production and nutrient cycling in sediments with benthic microalgae and transient accumulation of macroalgae. *Limnol Oceanog* 48:2138–2150
- Dayton PK, Watson D, Palmisano A, Barry JP, Oliver JS, Rivera D (1986) Distribution patterns of benthic microalgal standing stock at McMurdo Sound, Antarctica. *Polar Biol* 6:207–213
- Eicken H, Lange MA, Dieckmann DS (1991) Spatial variability of sea ice properties in the northwestern Weddell Sea. *J Geophys Res* 96:10603–10615
- Flameling IA, Kromkamp J (1998) Light dependence of quantum yields for PSII charge separation and oxygen evolution in eucaryotic algae. *Limnol Oceanog* 43:284–297
- Genty B, Briantias JM, Baker NR (1989) The relationship between the quantum yield of photosynthetic electron transport and quenching of chlorophyll fluorescence. *Biochem Biophys Acta* 990:87–92
- Gilbert NS (1991) Primary production by benthic microalgae in near shore marine sediments of Signey Island, Antarctica. *Polar Biol* 11:339–346
- Glud RN, Kuhl M, Wenzhöfer F, Rysgaard S (2002a) Benthic microphytes of a high arctic fjord: Importance for ecosystem primary production. *Mar Ecol Prog Ser* 238:15–29
- Glud RN, Rysgaard S, Kuhl M (2002b) A laboratory study of O₂ dynamics and photosynthesis in ice algal communities: quantification by microsensors, O₂ exchange rates, C14 incubations and a PAM fluorometer. *Aquatic Microbial Ecol* 27:301–311
- Grose M, McMinn A (2003) Algal biomass in east Antarctic pack ice: how MUCH is in the east? In: Huiskes AHL, Gieskes WWC, Rozema J, Schorno RML, An der Vies SM, Wolff WJ (eds) Antarctic biology in a global context. Proceedings of the VIIIth International Biology Symposium, 27 August–1 September 2001, Vrije Universiteit, Amsterdam, pp 21–25
- Horner RA, Schrader GC (1982) Relative contribution of ice algae, phytoplankton and benthic microalgae to primary production in nearshore regions of the Beaufort Sea. *Arctic* 35:485–503
- Jorgensen BB, Marais Des (1990) The diffusive boundary layer of sediments: oxygen microgradients over a microbial mat. *Limnol Oceanog* 35:1343–1355
- Jorgensen BB, Revsbech NP (1985) Diffusive boundary layers and the oxygen uptake of sediments and detritus. *Limnol Oceanog* 30:111–122
- Jorgensen BB, Revsbech NP, Cohen Y (1983) Photosynthesis and structure of benthic microbial mats: microelectrode and SEM studies of four cyanobacterial communities. *Limnol Oceanog* 28:1075–1093
- Klimant I, Kuhl M, Glud RN, Holst G (1997) Optical measurement of oxygen and temperature in microscale: strategies and biological applications. *Sensors Actuators B* 38:29–37
- Knox G (2006) *Biology of the southern ocean*, 2nd edn. CRC Press, Boca Raton
- Kuhl M, Lassen C, Jorgensen BB (1994) Light penetration and light intensity in sandy marine sediments measured with irradiance and scalar irradiance fibre-optic microprobes. *Mar Ecol Prog Ser* 105:139–148
- Kuhl M, Glud RN, Borum J, Roberts R, Rysgaard S (2001) Photosynthetic performance of surface-associated algae below sea ice as measured with a pulse-amplitude-modulated (PAM) fluorometer and O₂ microsensors. *Mar Ecol Prog Ser* 223:1–14
- Legendre L, Ackley SF, Dieckmann GS, Gulliksen B, Horner R, Hoshiai T, Melnikov LA, Reeburgh WS, Spindler M, Sullivan CW (1992) Ecology of sea ice biota. 2. Global significance. *Polar Biol* 12:429–444
- Lewis MR, Smith JC (1983) A small volume short incubation time method for the measurement of photosynthesis as a function of incident irradiance. *Mar Ecol Prog Ser* 13:99–102
- Lizotte MP (2001) The contributions of sea ice algae to Antarctic marine primary production. *Amer Zool* 41:57–73
- Lorenzen J, Glud RN, Revesbech NP (1995) Impact of microsensor-caused changes in diffusive boundary layer thickness on O₂ profiles and photosynthetic rates in benthic communities of microorganisms. *Mar Ecol Prog Ser* 119:237–241
- McMinn A (1996) Preliminary investigation of the contribution of fast ice algae to the spring phytoplankton bloom in Ellis Fjord, eastern Antarctica. *Polar Biol* 16:301–307
- McMinn A, Ashworth C (1998) The use of oxygen microelectrodes to determine the net production by an Antarctic sea ice algal community. *Antarctic Sci* 10:39–44
- McMinn A, Hegseth EN (2004) Quantum yield and photosynthetic parameters of marine microalgae from the southern Arctic Ocean, Svalbard. *J Mar Biol Assoc UK* 85:865–871
- McMinn A, Hegseth EN (2007) Sea ice Primary productivity in the northern Barents Sea, spring 2004. *Polar Biol* 30:289–294
- McMinn A, Hodgson D (1993) Seasonal phytoplankton succession in Ellis Fjord, eastern Antarctica. *J Plank Res* 15:925–938
- McMinn A, Gibson J, Hodgson D, Aschmann J (1995) Nutrient limitation in Ellis Fjord, Antarctica. *Polar Biol* 15:269–276
- McMinn A, Ashworth C, Ryan K (1999) Growth and productivity of Antarctic sea ice algae under PAR and UV irradiances. *Bot Mar* 42:401–407
- McMinn A, Ashworth C, Ryan KG (2000a) In situ net primary productivity of an Antarctic fast ice bottom algal community. *Aquatic Microbial Ecol* 21:177–185
- McMinn A, Bleakley N, Steinburger K, Roberts D, Trenerry L (2000b) Effect of permanent sea ice cover and different nutrient regimes on the phytoplankton succession of fjords of the Vestfold Hills Oasis, eastern Antarctica. *J Plank Res* 22:287–303
- McMinn A, Ryan K, Gademann R (2003) Photoacclimation of Antarctic fast ice algal communities determined by pulse amplitude modulation (PAM) fluorometry. *Mar Biol* 143:359–367
- McMinn A, Runcie J, Riddle M (2004) The effect of seasonal sea ice break-out on the photosynthesis of benthic diatom mats at Casey, Antarctica. *J Phycol* 40:62–69
- McMinn A, Hirawake T, Hamaoka T, Hattori H, Fukuchi M (2005) Contribution of benthic microalgae to ice covered coastal ecosystems in northern Hokkaido, Japan. *J Mar Biol Assoc UK* 85:283–289
- McMinn A, Ryan KR, Ralph PJ, Pankowski A (2007) Spring sea ice photosynthesis, primary productivity and biomass distribution in eastern Antarctica, 2002–2004. *Mar Biol* 151:985–995
- Mikkelsen D, Rysgaard S, Glud RN (2008) Microalgal composition and primary production in Arctic sea ice: a seasonal study from Kobbefjord (Kangerluarsunnguaq), West Greenland. *Mar Ecol Prog Ser* 368:65–74
- Palmisano AC, Soohoo JB, Sullivan CW (1985) Photosynthesis-irradiance relationships in sea ice microalgae from McMurdo Sound, Antarctica. *J Phycol* 21:341–346
- Platt T, Gallegos CL, Harrison WG (1980) Photoinhibition of photosynthesis in natural assemblages of marine phytoplankton. *J Mar Res* 38:687–701

- Ralph PJ, Gademann R (2005) Rapid light curves: a powerful tool to assess photosynthetic activity. *Aquatic Bot* 82:222–237
- Revsbech NP, Ward DM (1983) Oxygen microelectrode that is insensitive to medium chemical composition: use in an acid microbial mat dominated by *Cyanidium caldarium*. *Appl Environ Microbiol* 45:755–759
- Revsbech NP, Jørgensen BB (1986) Microelectrodes: their use in microbial ecology. In: Marshall KC (ed) *Advances in microbial ecology*. Plenum, New York, pp 293–352
- Roberts J, McMinn A (2004) Marine diffusive boundary layers at high latitudes. *Limnol Oceanog* 49:934–939
- Rysgaard S, Glud RN (2007) Carbon cycling in Arctic marine ecosystems: case study—Young sound. *Medd Greenland Biosci* 58:216
- Rysgaard S, Kuhl M, Glud RN, Hansen JW (2001) Biomass, production and horizontal patchiness of sea ice algae in a high-Arctic fjord (Young Sound, NE Greenland). *Mar Ecol Prog Ser* 223:15–26
- Satoh H, Watanabe K (1988) Primary productivity in the fast ice area near Syowa Station, Antarctica, during spring and summer 1983/1984. *J Oceanog Soc Japan* 44:287–292
- Smith REH, Anning J, Clement P, Cota G (1988) Abundance and production of ice algae in resolute passage, Canadian Arctic. *Mar Ecol Prog Ser* 48:251–263
- Strickland JDH, Parsons TR (1972) *A practical handbook of seawater analysis* (2nd ed) Bull Fish Res Board Canada 167:1–311
- Trenerry LJ, McMinn A, Ryan KG (2002) In situ oxygen microelectrode measurements of bottom-ice algal production in McMurdo Sound. *Antarctica Polar Biol* 25:72–80
- Weiss RF (1970) The solubility of nitrogen, oxygen and argon in water and sea water. *Deep Sea Res* 17:721–735
- White AJ, Critchley C (1999) Rapid light curves: a new fluorescence method to assess the state of photosynthetic apparatus. *Photosynth Res* 59:63–72